

## Enhanced Laser Cooling of a Mechanical Resonator via Zero-Photon Detection

Evan A. Cryer-Jenkins<sup>1,\*</sup>, Kyle D. Major<sup>1,\*</sup>, Jack Clarke<sup>1</sup>, Georg Enzian<sup>1,2</sup>, Magdalena Szczykulska<sup>2</sup>, Jinglei Zhang<sup>3,4</sup>, Arjun Gupta<sup>1</sup>, Anthony C. Leung<sup>1</sup>, Harsh Rathee<sup>1</sup>, Andreas Ø. Sveta<sup>1</sup>, Anthony K. C. Tan<sup>1</sup>, Almut Beige<sup>5</sup>, Klaus Mølmer<sup>6</sup>, and Michael R. Vanner<sup>1,†</sup>

<sup>1</sup>Quantum Measurement Lab, Blackett Laboratory, Imperial College London, London SW7 2BW, United Kingdom

<sup>2</sup>Clarendon Laboratory, Department of Physics, University of Oxford, Oxford OX1 3PU, United Kingdom

<sup>3</sup>Institute for Quantum Computing, University of Waterloo, Waterloo, Ontario, N2L 3G1, Canada

<sup>4</sup>Department of Physics & Astronomy, University of Waterloo, Waterloo, Ontario, N2L 3G1, Canada

<sup>5</sup>The School of Physics and Astronomy, University of Leeds, Leeds LS2 9JT, United Kingdom

<sup>6</sup>Niels Bohr Institute, University of Copenhagen, Blegdamsvej 17, 2100 Copenhagen, Denmark



(Received 4 August 2024; accepted 17 December 2024; published 18 February 2025)

Throughout quantum science and technology, measurement is used as a powerful resource for nonlinear operations and quantum state engineering. In particular, single-photon detection is commonly employed for quantum-information applications and tests of fundamental physics. By contrast, and perhaps counter-intuitively, measurement of the absence of photons also provides useful information, and offers significant potential for a wide range of new experimental directions. Here, we propose and experimentally demonstrate cooling of a mechanical resonator below its laser-cooled mechanical occupation via zero-photon detection on the anti-Stokes scattered optical field and verify this cooling through heterodyne measurements. Our measurements are well captured by a stochastic master equation and the techniques introduced here open new avenues for cooling, quantum thermodynamics, quantum state engineering, and quantum measurement and control.

DOI: [10.1103/PhysRevLett.134.073601](https://doi.org/10.1103/PhysRevLett.134.073601)

**Introduction**—Cavity optomechanical laser cooling provides a rich avenue for research, and enables the preparation of low-entropy initial states of mechanical oscillators. Building on the pioneering work by Braginsky and colleagues [1], the thermal ground state has now been achieved via laser cooling in the optical [2] and microwave [3] domains. These achievements fueled numerous subsequent developments and laser cooling remains a very active area in cavity optomechanics [4]. Key to the performance of laser cooling is operation in the resolved sideband regime, where the cavity decay rate is much smaller than the mechanical angular frequency, i.e.,  $\kappa < \omega_m$ , to resonantly select the light-mechanics beam-splitter interaction. Outside the resolved-sideband regime, i.e.,  $\kappa > \omega_m$ , optical measurement-based techniques for cooling have been explored with a prominent example being feedback cooling [5,6], which has also now experimentally reached the thermal ground state [7]. An

undesirable consequence of both laser cooling and feedback cooling is the mechanical damping rate increases with increasing cooling. Other techniques for cooling utilize pulsed measurement approaches for mechanical position measurements beyond the standard quantum limit [8], which also enable mechanical squeezing and tomography [9]. Pulsed experiments employing these techniques are also progressing towards measurement-based cooling to the mechanical quantum noise level [10,11].

In quantum optics more broadly, measurement plays a central role for quantum-state engineering and quantum-information applications. Prominent examples include heralded single-photon generation via single-photon detection [12], single-photon addition and subtraction operations [13–15], and noiseless linear amplification [16]. While the majority of photon-counting schemes for state engineering utilize the presence of one or more photons, detecting the absence of photons may also modify a state. Such zero-photon detection has been considered in quantum optics as a tool for noiseless attenuation [17–20], for Gaussification of entanglement distillation outputs [21], for covert information sharing [22], and for optical state engineering and reconstruction [23–25]. The statistics of zero-photon events, often discounted in numerical and experimental protocols, also provide useful information for parameter estimation protocols [26], and quantum simulation [27]. Recent experimental works have also demonstrated that

\*These authors contributed equally to this work and are listed alphabetically.

†Contact author: [m.vanner@imperial.ac.uk](mailto:m.vanner@imperial.ac.uk); [www.qmeas.net](http://www.qmeas.net)

zero-photon detection after a beam-splitter interaction modifies the output optical field depending on the input photon statistics [28,29].

Quantum measurement techniques utilizing photon counting have also been recently employed in optomechanics applications [30,31] where correlations between Stokes-scattered and anti-Stokes-scattered fields have been explored [32,33], single- and multiphonon addition and subtraction operations to thermal mechanical states have been performed [34–36], and higher-order phonon correlations have been measured [37]. With the growing interest in optomechanical quantum measurement and with the continued interest in laser cooling in a wide range of optomechanical and Brillouin-scattering-based systems [38–40], a measurement-based scheme capable of cooling mechanical oscillators further than the limits of laser cooling therefore constitutes a valuable new tool.

In this Letter, we propose and experimentally demonstrate measurement-enhanced laser cooling of a mechanical oscillator via zero-photon detection of the anti-Stokes-scattered optical field. The enhancement to the cooling is increased with longer measurement times and is experimentally demonstrated for both a single time step and a sequence of time steps. The dynamics of the coupled optomechanical system, probed via heterodyne measurements of the anti-Stokes light, are well captured by a stochastic master equation, which allows the state of the mechanical mode to be determined from the measured light. The zero-photon-detection-enhanced laser cooling is also experimentally contrasted with the case of single-photon detection, which increases the mean mechanical occupation [34]. The effect of detection efficiency on both forms of measurement is explored, showing the reduction in achievable cooling via zero-photon detection as optical loss increases. The cooling technique introduced and demonstrated here combines the advantages of resolved-sideband laser cooling with measurement-based cooling and can be applied to many physical systems including optomechanics, electromechanics, atomic spin ensembles, and superconducting circuits. Moreover, this technique offers new tools for quantum measurement and control and to explore the interface of quantum mechanics and thermodynamics.

*Enhanced mechanical cooling via zero-photon detection*—To laser cool a mechanical oscillator, the optomechanical beam-splitter interaction is brought into resonance and the output frequency-upshifted light is unmonitored, i.e., a partial trace operation. To understand the cooling and heating effects described below, we note that this trace operation can be viewed as an average over detection of all photon numbers, including zero-, single-, and multiphoton detection events. As has been recently experimentally demonstrated, the detection of a single photon following the optomechanical beam-splitter interaction is a single-phonon subtraction operation that doubles the mean occupation of an initial thermal state [34–36], and multiphonon subtraction further increases the mean occupation [35].

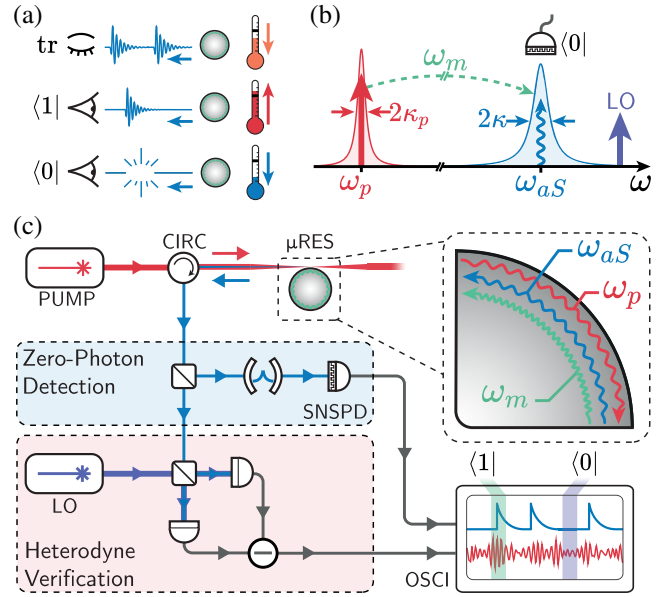


FIG. 1. Scheme and experimental schematic for zero-photon-measurement-enhanced laser cooling. (a) Cartoon of the effect of “no measurement” (corresponding to a trace operation), single-photon detection, and zero-photon detection on a thermal state. (b) The optical mode structure experimentally used to drive the Brillouin interaction. The pump mode is shown in red and the anti-Stokes mode in blue (offset by the Brillouin frequency in green). A local oscillator (LO) is located close in frequency to the anti-Stokes light. (c) Experimental schematic. A pump laser is coupled into a whispering-gallery-mode microresonator ( $\mu$ RES) and the backscattered anti-Stokes light is separated via an optical circulator (CIRC). The signal is then split in two: one portion is directed onto a superconducting nanowire single-photon detector (SNSPD) to perform zero-photon detection and heterodyne measurements are performed in a verification arm. The SNSPD and heterodyne signals are recorded on an oscilloscope (OSCI). Inset: A representation of the pump and counterpropagating anti-Stokes and mechanical (green) modes of the resonator.

Thus, as is represented schematically in Fig. 1(a), the zero-photon-detection events must constitute a cooling so laser cooling is achieved when all outcomes in the trace are averaged. Therefore, when the output light mode is instead monitored and zero-photon-detection events are used for heralding, the cooling is enhanced beyond standard laser cooling. This enhancement to laser cooling can also be understood from a Bayesian perspective due to the state-dependent measurement outcome probability. Mechanical states with larger excitations are more likely to generate photons and thus be excluded by zero-photon detection, and conversely, mechanical states with lower excitations are more likely to not generate a photon and are thus retained in the heralding process.

To see this quantitatively, we model the optomechanical interaction using the beam-splitter Hamiltonian  $H_{aS} = \hbar G(ab^\dagger + a^\dagger b)$ , where  $a$  and  $b$  are the annihilation

operators of the optical anti-Stokes and mechanical modes, respectively, and  $G$  is the linearized optomechanical coupling rate. The detection of  $n$  photons after a short anti-Stokes interaction of duration  $\tau$  is described by the measurement operator  $\Upsilon_n^{(aS)} = \langle n | e^{-iH_{aS}\tau/\hbar} | 0 \rangle \propto [\cos(G\tau)]^{b^\dagger b} b^n$ . Looking at the two parts to this measurement operator,  $b^n$  describes  $n$ -phonon subtraction and, crucially to this work, the term  $[\cos(G\tau)]^{b^\dagger b}$  present for zero-photon detection, when applied to a thermal state yields a new thermal state with a reduced thermal occupation. In order to model a time-continuous interaction, open-system dynamics, and measurements, we employ a stochastic master equation (SME) approach. By considering a series of short interactions and photon-counting measurements, and taking the limit  $\tau \rightarrow dt$  allows one to derive the SME

$$\begin{aligned} d\rho = & -\frac{i}{\hbar} [H_{aS}, \rho] dt + \mathcal{G}[a] \rho dN - \eta \kappa_{\text{ex}} \mathcal{H}[a^\dagger a] \rho dt \\ & + 2\kappa_{\text{ex}}(1 - \eta) \mathcal{D}[a] \rho dt + 2\kappa_{\text{in}} \mathcal{D}[a] \rho dt \\ & + 2\gamma(\bar{N} + 1) \mathcal{D}[b] \rho dt + 2\gamma\bar{N} \mathcal{D}[b^\dagger] \rho dt. \end{aligned} \quad (1)$$

Here,  $\eta$  is the total optical detection efficiency from outside the cavity to the photon counter,  $\kappa_{\text{ex}}(\kappa_{\text{in}})$  is the external (intrinsic) amplitude coupling (decay) rate of the cavity mode,  $\gamma$  is the amplitude decay rate of the mechanical mode,  $\bar{N}$  is the occupation of the mechanical thermal environment, and the superoperators are given by  $\mathcal{G}[O]\rho = O\rho O^\dagger / \langle O^\dagger O \rangle - \rho$ ,  $\mathcal{H}[O]\rho = O\rho + \rho O^\dagger - \langle O + O^\dagger \rangle \rho$ , and  $\mathcal{D}[O]\rho = O\rho O^\dagger - \frac{1}{2}\{O^\dagger O, \rho\}$ . Further, the stochastic increment  $dN = 0$  or  $1$  for a zero- or single-photon detection event and so  $dN^2 = dN$ . During each  $dt$ , zero-photon and single-photon detection events occur with probabilities  $\mathcal{P}_0 = 1 - 2\eta\kappa_{\text{ex}}\langle a^\dagger a \rangle dt$ , and  $\mathcal{P}_1 = 2\eta\kappa_{\text{ex}}\langle a^\dagger a \rangle dt$ , respectively, and one can see that heralding via zero-photon detection has a considerably more favorable probability compared to single-photon detection. For more details and further theoretical studies using this SME, see our companion article to this work, Ref. [41].

*Experimental setup*—We implement and verify the effect of zero-photon detection using Brillouin scattering in a 280  $\mu\text{m}$  diameter fused-silica microsphere resonator operating at room temperature and coupled using a tapered optical fiber. As illustrated in Fig. 1(b), we utilize two cavity modes spaced by the acoustic frequency  $\omega_m/2\pi = 10.85$  GHz to select and resonantly drive the anti-Stokes process. Utilizing a pair of cavity modes in this manner also ensures that the Stokes process is suppressed.

A schematic of the optical setup is shown in Fig. 1(c). Light from a continuous-wave pump laser at 1550 nm is sent through a circulator and is evanescently coupled into the microresonator. The transmitted pump field is used to characterize the optical modes and lock the pump laser to a cavity resonance via Pound-Drever-Hall frequency stabilization. The pump cavity mode used in this work has a

linewidth of  $2\kappa_p/2\pi = 6.1$  MHz and the anti-Stokes mode has a linewidth  $2\kappa/2\pi = 45.2$  MHz, with an external coupling rate of  $2\kappa_{\text{ex}}/2\pi = 10.1$  MHz, full-widths-at-half-maxima. The mechanical linewidth is  $2\gamma/2\pi = 45$  MHz, which is in good agreement with previous measurements and bulk decay rates in amorphous silica [42,43]. The pump-enhanced coupling rate is approximately  $G/2\pi = 3.3$  MHz for an input pump power of 0.37 mW, yielding a modest cooperativity of  $C = G^2/\kappa\gamma = 0.02$ . The photon-counting detection efficiency from the cavity output, including optical losses, is up to  $\eta = 0.32\%$  depending on the filtering configuration, and the efficiency of the heterodyne detection from cavity to detector is  $\eta_{\text{het}} = 29\%$ . Both of these efficiencies were estimated by measurement of optical path losses and are consistent with SME simulations.

The backscattered anti-Stokes light couples back into the tapered fiber, is separated from the counterpropagating pump by a circulator, and then split so that half the light is measured by a superconducting nanowire single-photon detector (SNSPD) following spectral filtering, and the remaining half is measured via heterodyne detection. Low optical powers were utilized in this experiment to avoid multiphoton detection by the SNSPD. We recorded an average photon detection rate of  $\sim 10^5$  s $^{-1}$ , which is well above the dark count rate observed of  $\lesssim 10$  s $^{-1}$ . The heterodyne and SNSPD signals are recorded on an oscilloscope with a 1.25 GHz sampling rate. The nanowire rise time is  $\sim 100$  ps and the oscilloscope sampling time is 0.8 ns, which are shorter than all relevant timescales in this experiment so photon-counting well approximates an instantaneous measurement. We record  $1.5 \times 10^7$  heterodyne and corresponding SNSPD time traces of 200 ns duration. We then digitally filter the measured heterodyne signals and determine the heterodyne statistics conditioned on the SNSPD measurement record. The heterodyne variance is scaled to intracavity optical occupation and compared to the associated mean photon number and phonon number obtained from the SME. We'd like to clarify here that the SME is not used for data analysis but rather gives a theoretical prediction for what our experiment observes. Measurement over a single time sample and a string of multiple time samples, i.e., an SNSPD measurement record, are examined.

*Results and discussion*—Figure 2(a) shows the mean phonon number  $\langle b^\dagger b \rangle$  and intracavity photon number  $\langle a^\dagger a \rangle$  obtained from the heterodyne signals for the three cases of “no measurement,” single-photon detection, and zero-photon detection over a single time sample. The no-measurement trace shows occupations that are constant in time, equal to the laser-cooling steady-state occupations. The traces corresponding to single-photon detection demonstrate an approximate doubling in the optical occupation and an accompanying increase in the mean phonon number. As this experiment does not operate in the adiabatic regime where  $\kappa_{\text{ex}}$  is larger than all other relevant rates, the increase



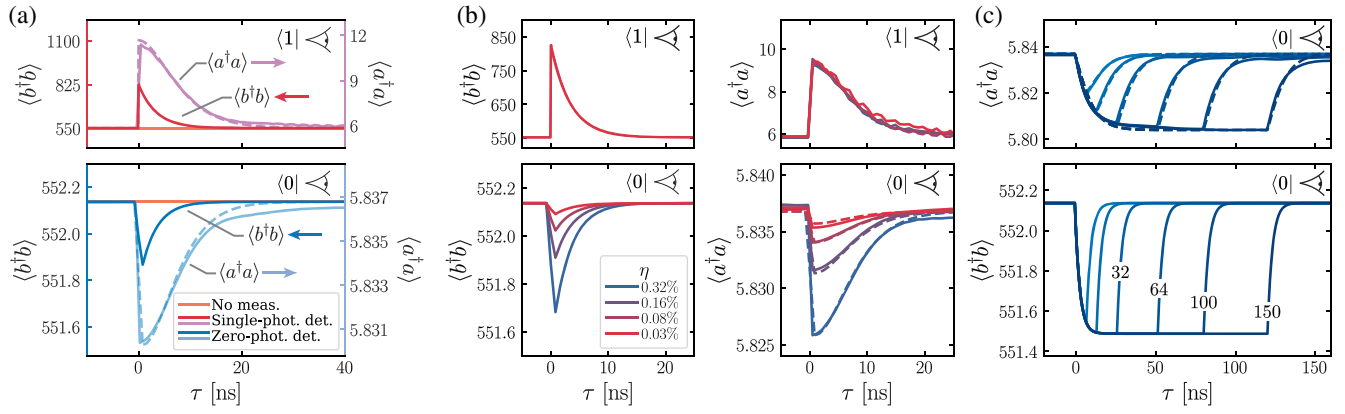


FIG. 2. Experimental observations of zero-photon-detection-enhanced laser cooling and dynamics associated with the photon-counting measurement record. (a) Plots of the mechanical and optical mean occupations for single-photon detection (upper row) and zero-photon detection (lower row) over a single time step as a function of time  $\tau$  from the measurement. The left vertical axes are the mechanical mean occupations and the right vertical axes are the optical mean occupations. (b) Plots illustrating the impact of efficiency on the single-photon and zero-photon cases for a range of efficiencies implemented by including additional attenuation. The scaling with efficiency for zero-photon detection is observed whereas the single-photon case remains unaffected and the four curves overlap. (c) Enhanced mechanical cooling through continuous zero-photon detection. Plot of the intracavity mean photon number (upper row) obtained from the experimental heterodyne data (solid lines) overlaid with the prediction made by the SME (dashed lines) using the experimental parameters summarized in [44]. The corresponding mechanical occupation (lower row) showing the improved cooling performance with measurement time. The lengths of the zero-photon detection strings used are 8, 16, 32, 64, 100, and 150 (in units of 0.8 ns). An efficiency  $\eta$  of 0.19% is used in plots (a) and (c), and the efficiencies for (b) are given in the legend.

in mean phonon number is less than a factor of 2. The small deviation from optical doubling is attributed to imperfect filtering of backscattered pump light and mode mismatch between the two detection arms. The plots for zero-photon detection illustrate a reduction from the laser-cooling occupations, demonstrating the enhancement beyond laser cooling. The experimental dynamics observed are in good agreement with the prediction made by the SME, which is also equivalent to the measurement-operator approach for this single-time-step case.

The impact of detection efficiency on zero-photon-measurement-enhanced laser cooling is examined by including optical attenuators prior to the SNSPD. For a single time sample, the depth of the enhanced cooling observed [cf. Fig. 2(b)] scales linearly with  $\eta$  as is predicted by our model [44]. By contrast, in the limit of low dark counts, the change in the state following single-photon detection does not depend on the detection efficiency, rather, this just affects the heralding probability. Note, a higher efficiency is employed for the measurement in Fig. 2(b) than in Figs. 2(a) and 2(c) by using less spectral filtering. This approach improves the performance of the zero-photon-detection-enhanced laser cooling but degrades the quality of the single-photon measurement as there are more false positives due to deleterious backscattered pump light.

Beyond zero-photon detection over a single time sample, this measurement-based cooling strategy may be further improved by implementing continuous zero-photon detection as illustrated in Fig. 2(c). Strings of zero-photon detection for up to 150 consecutive time steps (of 0.8 ns) are utilized, illustrating an improved cooling up to a limit

where heating rates balance information extracted from the system. To find the probability to successfully observe a string of zero-photon detection events, one may multiply the probabilities  $\mathcal{P}_0$  at every time step. Performing this continuous-time zero-photon detection for the modest cooperativity in this experiment, the mechanical occupation was reduced by a further 11.1% beyond laser cooling, which is heralded with a 98% probability for the 32 string case and 92% probability for the 150 string case. These heralding probabilities may be compared with the probability to detect a single photon from the laser-cooled steady state, which is 0.057% at any time step. Thus, our zero-photon detection scheme offers a more favorable heralding probability in contrast to click-based heralding approaches. For a given efficiency, the limit of cooling via continuous zero-photon detection is reached for a strongly overcoupled cavity, i.e.  $\kappa = \kappa_{\text{ex}}$ . When these conditions are met, the measurement-enhanced laser cooling gives a mechanical occupation of  $\bar{n}_{\text{lim}} = \left[ -(1+C) + \sqrt{(1+C)^2 + 4\eta\bar{N}C} \right] / 2\eta C$  [44]. In this regime, taking  $C = 0.02$  and  $\bar{N} = 558$  from our experiment, the laser-cooled occupation is  $\bar{n}_{\text{LC}} = \bar{N}/(1+C) = 547$  and the zero-photon-detection-enhanced occupation reduces to  $\bar{n}_{\text{lim}} = 143$  as  $\eta \rightarrow 1$ , which corresponds to 26% of the laser-cooled occupation. Furthermore, the contribution to cooling via zero-photon detection relative to standard laser cooling is maximum when  $C = 1$ , which, for the initial occupation of our experiment, gives  $\bar{n}_{\text{lim}} = 23$  as  $\eta \rightarrow 1$ , or approximately 8% of the laser-cooled occupation.

*Conclusions and outlook*—We propose and experimentally demonstrate the enhancement of laser cooling of a

mechanical mode via zero-photon detection of the frequency-upshifted optical field. The enhanced cooling is well described by a stochastic master equation, which captures the enhancement with a sequence of time steps of the measurement. The effects of detection inefficiency are understood and experimentally explored, as well as being contrasted against the loss-resilient effects of single-photon detection. The final occupation of the enhanced laser cooled state scales favorably with cooperativity and detection efficiency, and thus, improvements to these quantities result in a greatly improved cooling performance. For instance, for lower mechanical-frequency systems with larger thermal populations such as mechanical membranes [45] and forward Brillouin scattering [46], the effect is also significantly increased and can represent a significant advantage over conventional laser cooling alone for practical heralding probabilities. More generally, for high efficiency and cooperativity, to reduce the mean thermal occupation using zero-photon detection below a target value  $\bar{n}_*$  requires that the laser-cooled state has an occupation below  $\bar{n}_{\text{LC}} = \bar{n}_*^2 + \bar{n}_*$ . Indeed, to achieve  $\bar{n}_* < 1$  one requires laser cooling to  $\bar{n}_{\text{LC}} < 2$ , which is now achieved by several experimental platforms including optomechanical crystals [2,38], toroidal microresonators [47], and membranes [39]. Taking the parameters from Ref. [47] as an example, which performed laser cooling from 197 to 1.7 mean thermal phonons, employing zero-photon detection in that experiment could have enabled a mean thermal occupation of 0.90 to be reached. Such reductions to the laser-cooled mechanical occupations at these low levels, even for  $\bar{n}_{\text{LC}} < 1$ , are especially valuable for quantum state engineering protocols that are sensitive to initial thermal occupation.

This work utilizes the counter-intuitive fact that a measurement of “nothing” can have a significant impact to the state of a physical system. The technique introduced here combines the advantages of resolved-sideband laser cooling with measurement-based cooling, can be readily employed by several experimental systems to enhance their laser cooling performance, and more immediately performed in systems and protocols where photon detection is already employed [30–37,48–51]. This technique will also be of particular value to experiments aiming to achieve low thermal occupations from higher-occupation initial states, relaxing requirements for cryogenic precooling. We would also like to highlight that the additional cooling provided by this technique does not degrade the mechanical linewidth, further increasing the versatility of this approach. Beyond enhancing laser cooling, the zero-photon-detection-based technique introduced here expands the tool set of measurement-based operations to mechanical states, provides a method to perform mechanical noiseless attenuation, and opens new avenues for studies of quantum thermodynamics, and quantum measurement and control.

*Acknowledgments*—We acknowledge useful discussions with Lewis A. Clark, Rufus Clarke, Artie Clayton-Major, Lars Freisem, Daniel Hodgson, Gerard J. Milburn, and John J. Price. This project was supported by UK Research and Innovation (MR/S032924/1, MR/X024105/1), the Engineering and Physical Sciences Research Council (EP/T031271/1, EP/P510257/1), the Science and Technology Facilities Council (ST/W006553/1), the Royal Society, and the Aker Scholarship.

- 
- [1] V. Braginski and A. Manukin, *Sov. Phys. JETP* **25**, 653 (1967).
  - [2] J. Chan, T. M. Alegre, A. H. Safavi-Naeini, J. T. Hill, A. Krause, S. Gröblacher, M. Aspelmeyer, and O. Painter, *Nature (London)* **478**, 89 (2011).
  - [3] J. D. Teufel, T. Donner, D. Li, J. W. Harlow, M. Allman, K. Cicak, A. J. Sirois, J. D. Whittaker, K. W. Lehnert, and R. W. Simmonds, *Nature (London)* **475**, 359 (2011).
  - [4] M. Aspelmeyer, T. J. Kippenberg, and F. Marquardt, *Rev. Mod. Phys.* **86**, 1391 (2014).
  - [5] S. Mancini, D. Vitali, and P. Tombesi, *Phys. Rev. Lett.* **80**, 688 (1998).
  - [6] P. F. Cohadon, A. Heidmann, and M. Pinard, *Phys. Rev. Lett.* **83**, 3174 (1999).
  - [7] M. Rossi, D. Mason, J. Chen, Y. Tsaturyan, and A. Schliesser, *Nature (London)* **563**, 53 (2018).
  - [8] V. B. Braginsky, Y. I. Vorontsov, and F. Y. Khalili, *JETP Lett.* **27**, 276 (1978).
  - [9] M. R. Vanner, I. Pikovski, G. D. Cole, M. S. Kim, Č. Brukner, K. Hammerer, G. J. Milburn, and M. Aspelmeyer, *Proc. Natl. Acad. Sci. U.S.A.* **108**, 16182 (2011).
  - [10] M. R. Vanner, J. Hofer, G. D. Cole, and M. Aspelmeyer, *Nat. Commun.* **4**, 2295 (2013).
  - [11] J. T. Muhonen, G. R. La Gala, R. Leijssen, and E. Verhagen, *Phys. Rev. Lett.* **123**, 113601 (2019).
  - [12] C. K. Hong and L. Mandel, *Phys. Rev. Lett.* **56**, 58 (1986).
  - [13] A. Ourjoumtsev, R. Tualle-Brouiri, J. Laurat, and P. Grangier, *Science* **312**, 83 (2006).
  - [14] J. S. Neergaard-Nielsen, B. M. Nielsen, C. Hettich, K. Mølmer, and E. S. Polzik, *Phys. Rev. Lett.* **97**, 083604 (2006).
  - [15] A. Zavatta, V. Parigi, and M. Bellini, *Phys. Rev. A* **75**, 052106 (2007).
  - [16] G.-Y. Xiang, T. C. Ralph, A. P. Lund, N. Walk, and G. J. Pryde, *Nat. Photonics* **4**, 316 (2010).
  - [17] M. Mičuda, I. Straka, M. Miková, M. Dušek, N. J. Cerf, J. Fiurášek, and M. Ježek, *Phys. Rev. Lett.* **109**, 180503 (2012).
  - [18] C. N. Gagatsos, J. Fiurášek, A. Zavatta, M. Bellini, and N. J. Cerf, *Phys. Rev. A* **89**, 062311 (2014).
  - [19] R. A. Brewster, I. C. Nodurft, T. B. Pittman, and J. D. Franson, *Phys. Rev. A* **96**, 042307 (2017).
  - [20] W. Ye, H. Zhong, Q. Liao, D. Huang, L. Hu, and Y. Guo, *Opt. Express* **27**, 17186 (2019).
  - [21] D. E. Browne, J. Eisert, S. Scheel, and M. B. Plenio, *Phys. Rev. A* **67**, 062320 (2003).
  - [22] U. Zanforlin, G. Tatti, J. Jeffers, and G. S. Buller, *Phys. Rev. A* **107**, 022619 (2023).

- [23] K. Banaszek and K. Wódkiewicz, *Phys. Rev. Lett.* **76**, 4344 (1996).
- [24] M. S. Kim, *Phys. Rev. A* **56**, 3175 (1997).
- [25] G. Zambra, A. Andreoni, M. Bondani, M. Gramegna, M. Genovese, G. Brida, A. Rossi, and M. G. A. Paris, *Phys. Rev. Lett.* **95**, 063602 (2005).
- [26] L. A. Clark, A. Stokes, and A. Beige, *Phys. Rev. A* **99**, 022102 (2019).
- [27] S. C. Wein, *Phys. Rev. A* **109**, 023713 (2024).
- [28] C. M. Nunn, J. D. Franson, and T. B. Pittman, *Phys. Rev. A* **104**, 033717 (2021).
- [29] C. M. Nunn, J. D. Franson, and T. B. Pittman, *Phys. Rev. A* **105**, 033702 (2022).
- [30] K. Børkje, A. Nunnenkamp, and S. M. Girvin, *Phys. Rev. Lett.* **107**, 123601 (2011).
- [31] M. R. Vanner, M. Aspelmeyer, and M. S. Kim, *Phys. Rev. Lett.* **110**, 010504 (2013).
- [32] K. Lee, B. Sussman, M. Sprague, P. Michelberger, K. Reim, J. Nunn, N. Langford, P. Bustard, D. Jaksch, and I. Walmsley, *Nat. Photonics* **6**, 41 (2012).
- [33] R. Riedinger, S. Hong, R. A. Norte, J. A. Slater, J. Shang, A. G. Krause, V. Anant, M. Aspelmeyer, and S. Gröblacher, *Nature (London)* **530**, 313 (2016).
- [34] G.ENZIAN, J. J. Price, L. Freisem, J. Nunn, J. Janousek, B. C. Buchler, P. K. Lam, and M. R. Vanner, *Phys. Rev. Lett.* **126**, 033601 (2021).
- [35] G.ENZIAN, L. Freisem, J. J. Price, A. O. Svela, J. Clarke, B. Shajilal, J. Janousek, B. C. Buchler, P. K. Lam, and M. R. Vanner, *Phys. Rev. Lett.* **127**, 243601 (2021).
- [36] R. N. Patel, T. P. McKenna, Z. Wang, J. D. Witmer, W. Jiang, R. Van Laer, C. J. Sarabalis, and A. H. Safavi-Naeini, *Phys. Rev. Lett.* **127**, 133602 (2021).
- [37] Y. S. S. Patil, J. Yu, S. Frazier, Y. Wang, K. Johnson, J. Fox, J. Reichel, and J. G. E. Harris, *Phys. Rev. Lett.* **128**, 183601 (2022).
- [38] L. Qiu, I. Shomroni, P. Seidler, and T. J. Kippenberg, *Phys. Rev. Lett.* **124**, 173601 (2020).
- [39] R. W. Peterson, T. P. Purdy, N. S. Kampel, R. W. Andrews, P.-L. Yu, K. W. Lehnert, and C. A. Regal, *Phys. Rev. Lett.* **116**, 063601 (2016).
- [40] L. Blázquez Martínez, P. Wiedemann, C. Zhu, A. Geilen, and B. Stiller, *Phys. Rev. Lett.* **132**, 023603 (2024).
- [41] J. Clarke, E. A. Cryer-Jenkins, A. Gupta, K. D. Major, J. Zhang, G.ENZIAN, M. Szczykulska, A. C. Leung, H. Rathee, A. K. C. Tan, A. Ø. Svela, A. Beige, K. Mølmer, and M. R. Vanner, companion paper, *Phys. Rev. A* **111**, 023516 (2025).
- [42] R. Boyd, *Nonlinear Optics* (Academic Press Inc., San Diego, CA, 1992).
- [43] G.ENZIAN, M. Szczykulska, J. Silver, L. Del Bino, S. Zhang, I. A. Walmsley, P. Del'Haye, and M. R. Vanner, *Optica* **6**, 7 (2019).
- [44] See Supplemental Material at <http://link.aps.org/supplemental/10.1103/PhysRevLett.134.073601> for further experimental and theoretical details.
- [45] M. B. Kristensen, N. Kralj, E. C. Langman, and A. Schliesser, *Phys. Rev. Lett.* **132**, 100802 (2024).
- [46] G. Bahl, M. Tomes, F. Marquardt, and T. Carmon, *Nat. Phys.* **8**, 203 (2012).
- [47] E. Verhagen, S. Deléglise, S. Weis, A. Schliesser, and T. J. Kippenberg, *Nature (London)* **482**, 63 (2012).
- [48] J. D. Cohen, S. M. Meenehan, G. S. MacCabe, S. Gröblacher, A. H. Safavi-Naeini, F. Marsili, M. D. Shaw, and O. Painter, *Nature (London)* **520**, 522 (2015).
- [49] E. A. Cryer-Jenkins, G.ENZIAN, L. Freisem, N. Moroney, J. J. Price, A. Ø. Svela, K. D. Major, and M. R. Vanner, *Optica* **10**, 1432 (2023).
- [50] T. J. Milburn, M. S. Kim, and M. R. Vanner, *Phys. Rev. A* **93**, 053818 (2016).
- [51] I. Galinskiy, G.ENZIAN, M. Parniak, and E. S. Polzik, *Phys. Rev. Lett.* **133**, 173605 (2024).